Froghopper-inspired direction-changing concept for miniature jumping robots

2016 Bioinspir. Biomim. 11 056015

(http://iopscience.iop.org/1748-3190/11/5/056015)

Bioinspiration & Biomimetics

CrossMark

RECEIVED
22 March 2016

REVISED
15 June 2016

ACCEPTED FOR PUBLICATION
9 August 2016

PUBLISHED
14 September 2016

PAPER

Froghopper-inspired direction-changing concept for miniature jumping robots

Gwang-Pil Jung and Kyu-Jin Cho

School of Mechanical and Aerospace Engineering/Institute of Advanced Machines and Design, Seoul National University, Seoul 151-742, Korea

E-mail: kjcho@snu.ac.kr

Keywords: jumping mechanism, jumping robot, direction change, froghopper

Supplementary material for this article is available online

Abstract

To improve the maneuverability and agility of jumping robots, several researchers have studied steerable jumping mechanisms. This steering ability enables robots to reach a particular target by controlling their jumping direction. To this end, we propose a novel direction-changing concept for miniature jumping robots. The proposed concept allows robots to be steerable while exerting minimal effects on jumping performance. The key design principles were adopted from the froghopper's power-producing hind legs and the moment cancellation accomplished by synchronized leg operation. These principles were applied via a pair of symmetrically positioned legs and conventional gears, which were modeled on the froghopper's anatomy. Each leg has its own thrusting energy, which improves jumping performance by allowing the mechanism to thrust itself with both power-producing legs. Conventional gears were utilized to simultaneously operate the legs and cancel out the moments that they induce, which minimizes body spin. A prototype to verify the concept was built and tested by varying the initial jumping posture. Three jumping postures (synchronous, asynchronous, and single-legged) were tested to investigate how synchronization and moment cancelling affect jumping performance. The results show that synchronous jumping allows the mechanism to change direction from –40° to 40°, with an improved take-off speed. The proposed concept can only be steered in a limited range of directions, but it has potential for use in miniature jumping robots that can change jumping direction with a minimal drop in jumping performance.

1. Introduction

Jumping locomotion has been widely employed for small-scale robots to overcome their size limitations. The ability to jump high despite a small body size allows these robots to overcome large obstacles and distances. To achieve high jumping performance, a variety of mechanisms have been applied, such as an escapement mechanism using a cam or gear (Kovac *et al* 2008, Li *et al* 2008), an active clutch (Woodward and Sitti 2014), torque-reversal (Noh *et al* 2012, Koh *et al* 2015), a one-way bearing (Zhao *et al* 2014), an inchworm motor (Gerratt and Bergbreiter 2013), and combustion (Tolley *et al* 2014, Bartlett *et al* 2015). These mechanisms have shown great jumping performance, but most of them focus on the jumping locomotion itself.

To improve the maneuverability of milli-scale jumping robots, several researchers have studied the effect of adding a steering method. When steering is added, small jumping robots are able to reach a target by, for example, controlling their jump direction. Previously, Kovač *et al* (Kovač *et al* 2010) classified steering mechanisms into four working principles: using wheels to rotate the whole body, shifting the center of gravity, using a foot to rotate the whole body, and using a rotating jumping mechanism inside of a cage. Stoeter *et al* (Stoeter *et al* 2002) made a 'Scout robot' that maneuvers with a wheel and jumps with a winch. This robot alters its location in the plane and jumps to open up movement in a three-dimensional (3D) space. Zhao *et al* (Zhao *et al* 2014) presented a 23.5 g single-motor-actuated steerable jumping robot. The robot has two steering gears that can contact the ground after

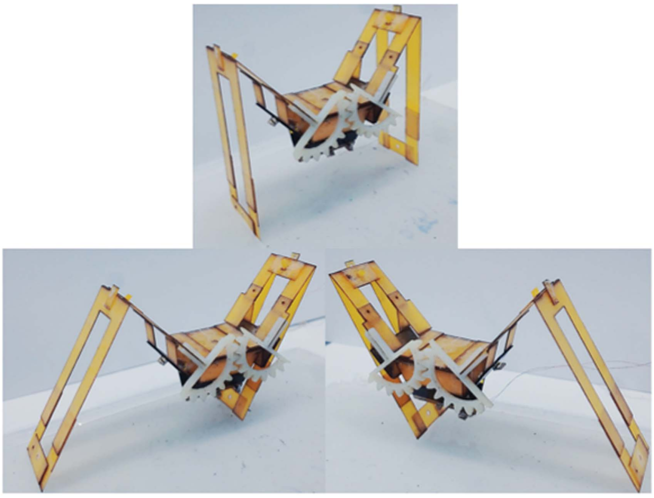

Figure 1. Froghopper-inspired direction-changing mechanism weighing 3.06 g, showing the initial positions for an upward jump (top), a rightward jump (bottom left), and a leftward jump (bottom right).

landing. The robot can change its jumping direction by rotating the gear that touches the ground first. In addition, the robot's two legs rotate in opposite directions, for self-righting. Weiss *et al* (Weiss 2001) proposed a 2.5 kg jumping robot using a piston-driven combustion chamber. This robot can change the location of its center of mass to control its jumping orientation. Armour *et al* (Armour *et al* 2007) proposed the 'Jollbot,' which can upright itself, roll, and change jump direction. A servomotor twists the robot's spherical shell so that its center of gravity changes and the main jumping axis leans. Burdick *et al* (Burdick and Fiorini 2003) employed an active steering mechanism using a ring gear at the foot of their robot that can rotate the whole body around the vertical axis. In the fully compressed position, a pinion gear driven by the primary motor contacts the ring gear and controls the steering angle. Kovač *et al* (Kovač *et al* 2010) proposed a 14 g jumping robot that can upright itself and steer. They installed a cage structure that allows the robot to passively upright itself by exerting gravitational force on the center of mass. Steering is accomplished by rotating the robot's body inside the cage using a motor and a double-guided axis.

These mechanisms have all succeeded in changing the jumping direction of a robot. In terms of jumping performance, however, some jumping robots perform poorly owing to the weight of the additional steering structures. To resolve this issue, we propose a novel concept for a direction-changing mechanism for miniature jumping robots, shown in figure 1. This mechanism not only enables a robot to change its jumping direction but also improves its jumping performance. The key design principles are adopted from two key features of froghoppers' jumping: power-producing hind legs and moment cancellation accomplished by synchronized jumping (Sutton and Burrows 2010).

Froghoppers change their jumping azimuth to escape from predators or to move from one position to another. Interestingly, their azimuth control is accomplished in a manner that minimizes needless rotation of the body and maximizes take-off speed as well. Froghoppers have a pair of hind legs, each of which has its own thrusting energy. By using two thrusting legs, froghoppers can achieve considerably high output power, up to 35 W g^{-1}. At the same time, the moments generated by both legs cancel each other out through synchronized leg operation, which reduces needless rotation.

These principles are applied in the proposed mechanism via a pair of symmetrically positioned legs and conventional gears (Burrows and Sutton 2013). The mechanism has a pair of symmetrically positioned legs that perform jumping, and each leg has its own thrusting energy. Thrusting the mechanism with two power-producing legs improves jumping performance. These two legs, however, should operate simultaneously since an operational timing difference would prevent the moments induced by the legs from cancelling each other out, resulting in unnecessary body spin. To avoid this, a pair of conventional gears is installed at both of the mechanism' legs to ensure synchronized leg operation.

In the following sections, the mechanics of the froghopper's steerable jumping and the design concepts derived from them are explained in detail. To analyze the motion of the jumping mechanism, free body diagrams of the leg components are derived. Several experiments on the effect of synchronous jumping, asynchronous jumping, and single-legged jumping on jumping performance are then described.

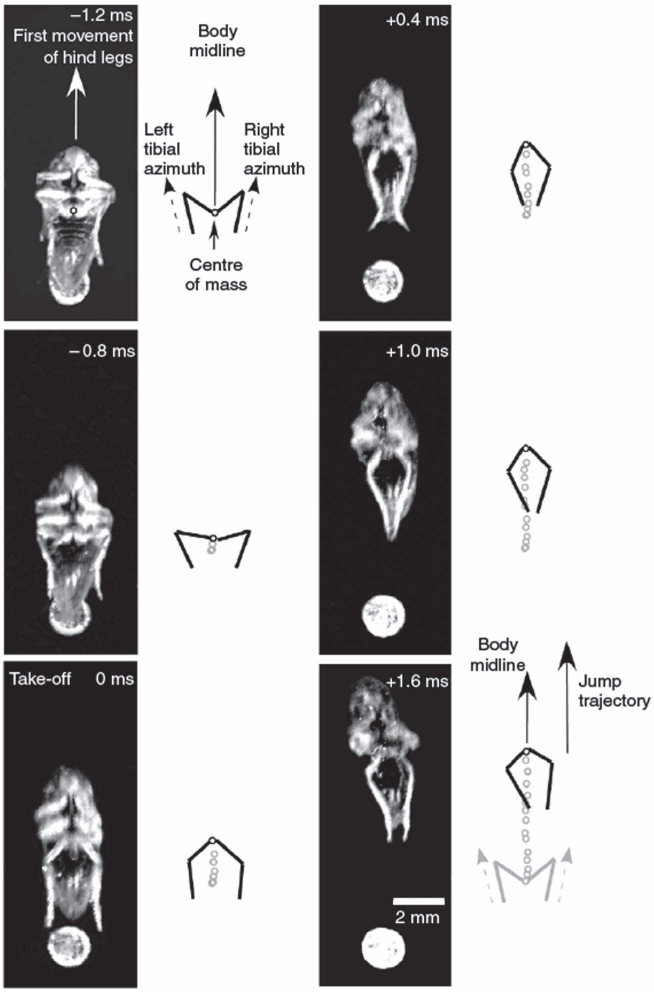

Figure 2. Take-off of the froghopper, *Philaenus spumarius,* viewed ventrally (5000 frames per second). The hind legs operate simultaneously, and this enables cancellation of moments induced by the legs, resulting in reduced body spin (adapted from Sutton *et al* 2010 *J. Exp. Biol.* **213** 1409, with permission of Sutton) (Sutton and Burrows 2010).

2. Design

2.1. Froghopper jumping

The froghopper, *Philaenus spumarius,* is well known for its amazing jumping performance. The froghopper takes off in 1.2 ms with a mean velocity of 2.8 m s^{-1} (Burrows 2003). This corresponds to an average output power of 35 W g^{-1}, which is much greater than that of locusts (0.45 W g^{-1}) (Bennet-Clark 1975) and fleas (14 W g^{-1}) (Sutton and Burrows 2011). This outperforming jump originates from a pair of hind trochanteral depressor muscles connecting the thorax to the trochanter. Before take-off, a pair of hind legs is levated and locked by a lateral protrusion. When fully levated, both legs start to depress, and the froghopper jumps within 1 ms as shown in figure 2 (Sutton and Burrows 2010).

Froghoppers control their jumping azimuth efficiently by means of the following principles (Sutton and Burrows 2010): prior alteration of tibiae orientation, moment cancellation generated by each hind leg, and synchronized depression of both hind legs. Froghoppers alter the orientation of their hind tibiae to jump toward a desired direction. This orientation corresponds to the jumping azimuth angle. Therefore, the azimuth direction can be estimated based on the initial posture.

When froghoppers take off, moments are generated by each hind leg. The left leg makes the body rotate in the clockwise direction, and the right leg does the opposite. These two generated moments in opposite directions greatly reduce rotation of the jumping body and increase useful kinetic energy. Moreover, both hind legs depress almost equally. Sutton and Burrows (Sutton and Burrows 2010) showed that both legs are synchronized to within 32 μs. This synchronous jump also enables efficient jumping by preventing the body from spinning unnecessarily.

2.2. Jumping mechanism design

Inspired by froghoppers, a novel concept for a direction control mechanism is proposed in this paper. The mechanism has a body at the center with one jumping leg located at each side, as shown in figure 3(a). Both

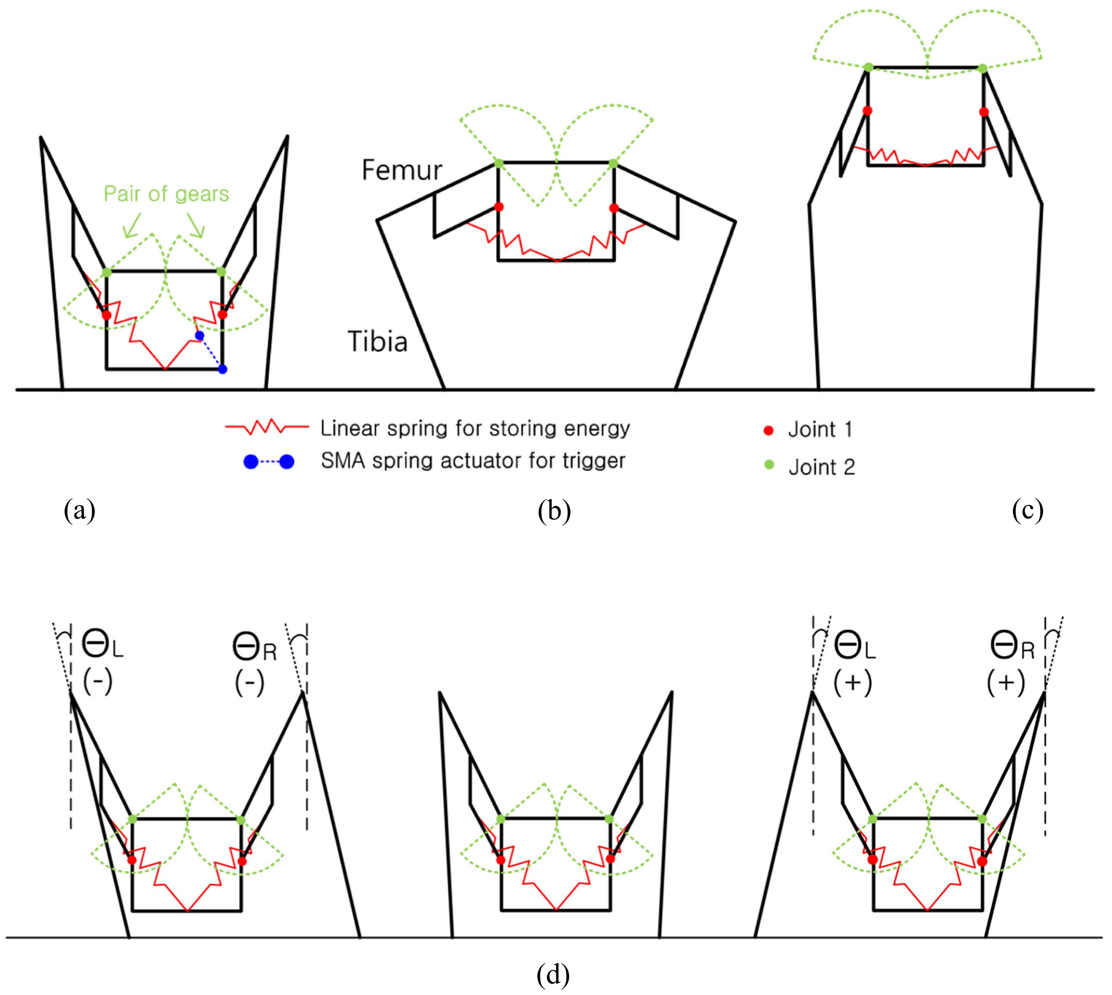

Figure 3. Schematic of the jumping mechanism (a) in the fully levated position, (b) in the middle of jumping, and (c) in the fully depressed position. (d) Schematic of the events involved in altering the initial posture.

jumping legs can move independently, and each leg has a linear spring to provide energy storage. A pair of gears is installed on the leg to synchronize depression of the legs during a jump. A triggering shape memory alloy (SMA) coil spring actuator is installed on the only right leg as shown in figure 3(a), but there is no problem with synchronous operation of both legs owing to the gears.

The proposed mechanism utilizes the torque reversal catapult mechanism (Noh *et al* 2012). When the linear spring in the right leg is pulled by the trigger and passes through joint 1, the right jumping leg starts to depress shortly afterward. At this moment, the gear installed on the right leg triggers the gear on the left leg, and jumping ensues. Both jumping legs are thus synchronized to within 2.38 ms, considering that take-off is filmed at 420 frames per second and both legs are synchronized within 1 frame. This synchronous jump continues until both jumping legs are fully depressed, as shown in figure 3(c).

Figure 3(d) shows how the mechanism changes the jumping direction by altering the robot's initial posture, just as real froghoppers do. The femorotibial joints freely rotate so that the mechanism can easily alter the initial orientation of the tibiae. Currently, actuators for altering the posture are not installed on the prototype since in this paper we focus on the feasibility test of whether this concept can be applied to miniature jumping robots.

3. Jumping direction analysis

To investigate how generated forces and moments affect jumping direction, free body diagrams and the corresponding equations are derived. The analysis makes the following assumptions for purposes of simplification: first, the torques generated by the linear springs at both sides of the mechanism are equal, and both legs operate synchronously. Second, the femorotibial joints have low stiffness and rotate freely.

The position of each tibia is directly related to the jump direction since the distal end of the tibia contacts the ground and receives the reaction force. The direction of this reaction force determines which way the mechanism moves. Therefore, the relation between

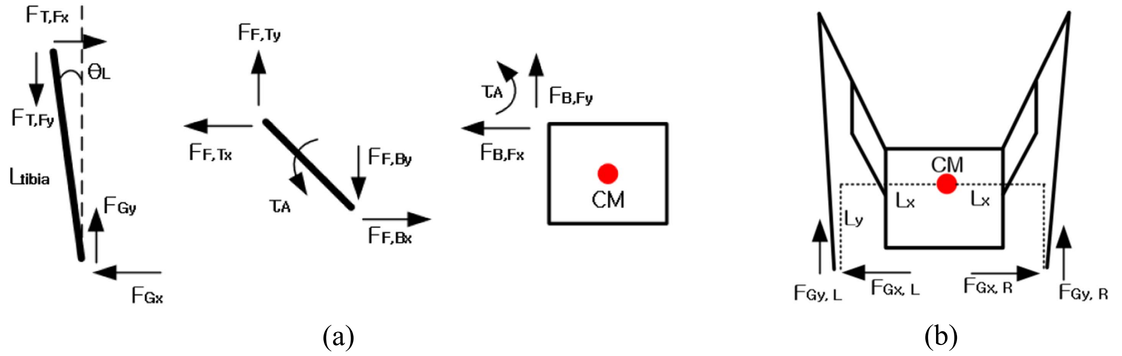

Figure 4. Free body diagrams (FBD) of the body and components. (a) FBD of tibia, femur, and body. (b) FBD of whole mechanism.

the reaction force exerted on the tibia and the initial angle of the tibia must be clarified.

As previously said, the mechanism changes jump direction by altering its initial posture. To clarify the relation between the initial posture and the jumping direction, free body diagrams of the tibia, the femur, and the body are derived as shown in figure 4. The internal forces cancel each other out according to the principle of action and reaction. The reaction force from the ground remains, and it exerts on the tibia.

Figure 4(a) shows the free body diagram of the tibia. The joint connecting the tibia and the femur has quite low stiffness and can be regarded as a freely rotating joint. Therefore, the femorotibial joint does not transmit the torque generated by the linear spring, and consequently net torque drops to almost zero. To satisfy this condition, the reaction force from the ground needs to generate zero torque, as follows:

$$L_{\text{tibia}} F_{G_x} \cos\theta_L - L_{\text{tibia}} F_{G_y} \sin\theta_L \approx 0, \qquad (1)$$

where L_{tibia} is the length of the tibia, θ_L is the angle of the left tibia, and F_{G_x} and F_{G_y} are the ground reaction force in the x and y directions, respectively.

Accordingly, the following relation can be derived:

$$\tan\theta_L = \frac{F_{G_x}}{F_{G_y}}. \qquad (2)$$

Equation (2) tells us that the direction of the reaction force is parallel to the direction of the tibia, just like in the froghopper (Sutton and Burrows 2010). That is, the direction of thrust force can be predicted by the posture of the tibia, which is how the jumping direction can be estimated. Given that an object moves in the direction that is specified by a force vector, we may accordingly predict jump direction by combining the direction of two force vectors generated by both tibiae:

$$\theta_{\text{Jump direction}} \approx \frac{\theta_L + \theta_R}{2},$$

where θ_L and θ_R are the angles of the left and right tibia, as indicated in figure 3(d).

In terms of the whole mechanism, only ground reaction forces exert external force on the mechanism.

Table 1. Mass budget.

Components	Quantity (ea.)	Mass (g)	Ratio to overall mass (%)
Gear	2	0.21	13.8
Body structure	1	0.85	30.0
Linear spring	2	0.19	12.5
Trigger SMA	1	0.19	6.25
Tibia	2	0.28	18.4
Femur	2	0.32	21.0
Total	—	3.06	100

Accordingly, the equation of rotating motion for the whole body is as follows:

$$I\ddot{\theta} = F_{G_y,R} L_x + F_{G_x,R} L_y - F_{G_y,L} L_x - F_{G_x,R} L_y, \qquad (3)$$

where L_x and L_y are the lengths between the center of mass and the contact point of the tibia and the ground, and $F_{G_y,R}$ and $F_{G_y,L}$ are the ground reaction force of the left and right leg in the y direction.

Since the overall shape of the mechanism is symmetrical, the moments generated by the reaction forces cancel each other out in equation (3): the first and second terms cause moment in a clockwise direction, while the third and fourth terms cause moment in a counter-clockwise direction. Consequently, the mechanism can take off with reduced body spin.

4. Fabrication and assembly

The proposed mechanism was fabricated using smart composite microstructures (Wood *et al* 2008) to make a lightweight but robust mechanism. The mechanism weighs 3.06 g, and the mass budget is shown in table 1. To strengthen the places where linear springs are connected and stress is concentrated, carbon–epoxy composite plates were used (figure 5(b)).

For energy storage, linear springs were employed. The linear spring used has a spring constant of 459 N m^{-1} and an original length of 9 mm. In the fully levated position, the spring is stretched 14.4 mm and stores the elastic energy of 6.67 mJ. 3D-printed (Objet 260, Stratasys Inc.) gears are used to synchronize

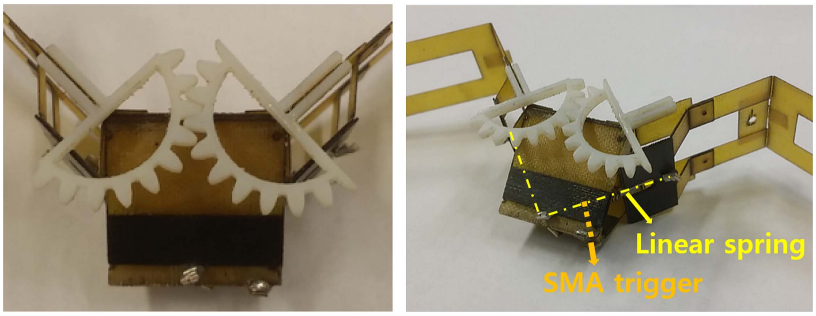

(a) (b)

Figure 5. (a) 3D-printed gears that enable a synchronous jump. (b) Linear springs for storing energy and an SMA actuator for triggering. The linear springs and the SMA actuator are located inside the body at the locations indicated by the dashed lines.

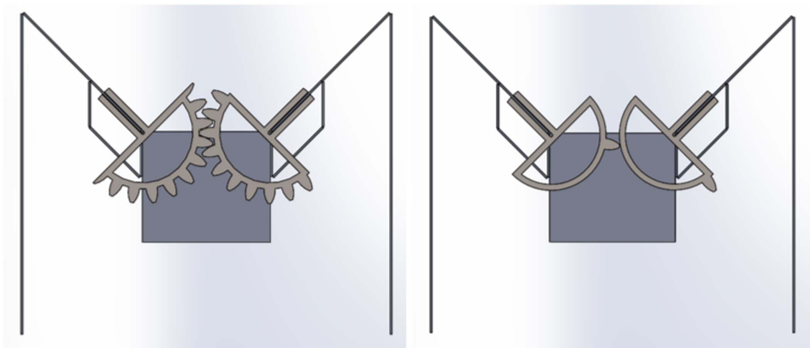

(a) (b)

Figure 6. Gears to control the activation time difference. The right leg operates first. (a) Gears for equal activation. (b) Gears for an activation time difference of 14.2 ms.

operation of the jumping legs. To reduce mass, the gears are designed as semicircles and are hollow. One gear is installed at each femur in a position such that the gears mesh, as shown in figure 5(a).

5. Experimental results

5.1. Methods

The main working principles that enable the proposed concept are the two power-producing legs for improving jumping performance and moment cancellation accomplished by synchronized leg operation. To investigate what happens when whether these principles are properly working or not, three kinds of jumping (synchronous, asynchronous, and single-legged) were tested. First of all, a synchronous jumping that satisfies both working principles was done to confirm the proposed concept. To observe a case when one power-producing leg is missing, single-legged jumping was tested by fixing the left leg and only operating the right leg. Asynchronous jumping was tested to observe how an operation timing difference affects jumping performance by setting up an activation time difference between the left and right legs.

To accomplish this, special timing gears were used to ensure a consistent activation time difference, as shown in figure 6. The single tooth on each of these gears is positioned to ensure that the left leg deploys after the right one at a consistent interval. When the SMA actuator triggers the right leg, only the right gear begins to rotate. After an interval of time, the tooth on the right gear contacts the tooth on the left gear, and the left leg is triggered. In the experiment, 14.2 ms of time difference always occurred.

To investigate the relationship between jump direction and the initial posture of the mechanism, several jumping experiments were conducted by altering the initial posture. Details of the selected initial postures are given in table 2. Three initial postures for jumping leftward, upward, and rightward were selected to test the full range of jump directions. Three jumps were done in each direction to check repeatability. The initial angles of the legs were measured prior to triggering the mechanism. Also, average values were given for the right leg and the left leg to allow actual jumping directions to be both predicted and compared.

Jumps were done on a polymer pad (Dragon Skin; Smooth-on, Inc., 1 mm thickness) to provide enough

Table 2. Initial posture of jumping legs.

Jump direction	Leftward			Upward			Rightward		
Experiment no.	1	2	3	1	2	3	1	2	3
Synchronous jump									
Initial angle of right leg (deg)	−27.1	−26.8	−27.9	1.9	1.5	1.1	26.5	27.6	26.7
Initial angle of left leg (deg)	−26.3	−27.2	−27.1	1.8	1.3	1.0	27.8	26.1	27.2
Avg. angle (deg)	−26.7	−27.0	−27.5	1.9	1.4	1.0	27.2	26.8	26.9
Asynchronous jump									
Initial angle of right leg (deg)	−27.2	−26.3	−27.0	3.6	1.1	2.5	26.5	27.2	26.8
Initial angle of left leg (deg)	−26.4	−27.9	−26.4	−0.4	−4.2	−3.8	26.1	26.1	27.1
Avg. angle (deg)	−26.8	−27.1	−26.7	1.5	−1.5	−0.6	26.3	26.7	27.0
Single-legged jump									
Initial angle of right leg (deg)	−27.1	−27.8	−27.0	0.4	0.7	−1.42	27.7	27.2	27.4
Initial angle of left leg (deg)	−26.3	−26.1	−26.7	2.3	1.7	3.98	26.4	26.7	26.3
Avg. angle (deg)	−26.7	−26.9	−26.8	1.4	1.2	1.28	27.0	26.9	26.9

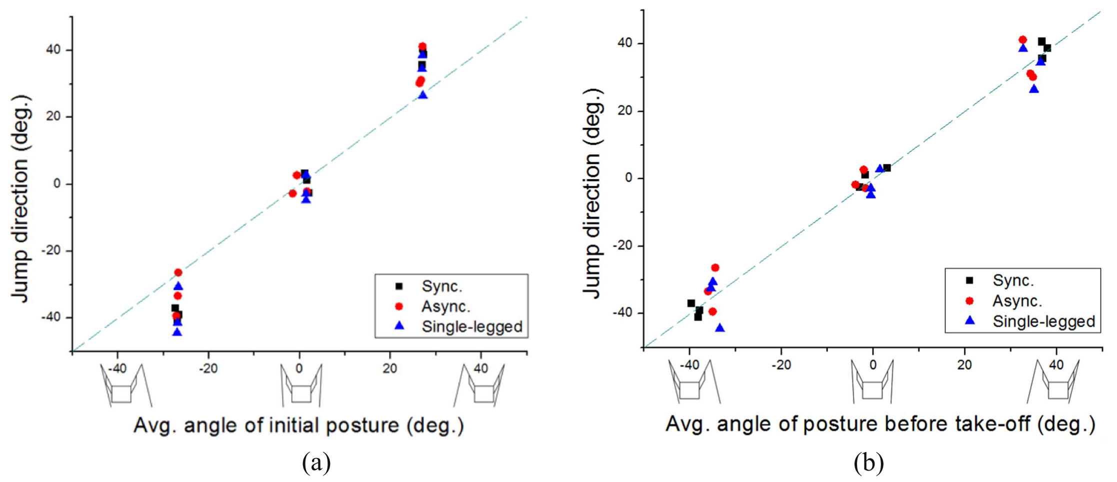

Figure 7. Relation between jump direction and (a) average angle of initial posture and (b) average angle before take-off. The dotted line is a linear fuction of $y = ax$, where $a = 1$.

friction to prevent slippage during jumping. To trigger the mechanism, the SMA actuator was activated via joule heating by 1.2 A from the external power supply. The jumping data was obtained with a high-speed camera (420 frames per second), and video analysis software (ProAnalyst; Excitex, Inc.) was used to analyze take-off velocity and take-off angular velocity for various jumping directions.

5.2. Jumping direction

Figure 7(a) shows that the jump direction depends on the average angle of the initial posture. The overall jump direction spreads from −44° to 41°. Basically, the jump direction corresponds to the sign of the average angle. For example, the mechanism jumps leftward when the average angle has negative value. If we compare the average angle and the jump direction, however, there is a slight difference between them. This is because the angle of the tibia changes during jumping, as shown in figure 8. The mechanism has a long femur, and therefore the position of the femorotibial joint changes a great deal. For example, the angle of the left tibia varies from 1.83° to −12.15° during depression of the leg, as shown in figure 8. Since the angle of the tibia changes, the direction of the ground reaction force also changes according to equation (2). Therefore, the jumping direction can be differed from the average angle of the initial posture.

To precisely check the relationship between jump direction and the posture of the mechanism, and specifically whether the angle of the tibia predicts jump direction, we measured the tibial angle 2.4 ms (1 frame) before take-off and compared the angle with the jump direction. Figure 7(b) shows the average angle just before take-off compared to jump direction. Unlike the average angle of the initial tibia posture, the tibial angle matches better with the jump direction, especially for synchronous jumps.

Neither asynchronous nor single-legged jumping have much effect on jump direction. In the single-legged case, there is about 11° of difference between jump direction and average angle when the mechanism

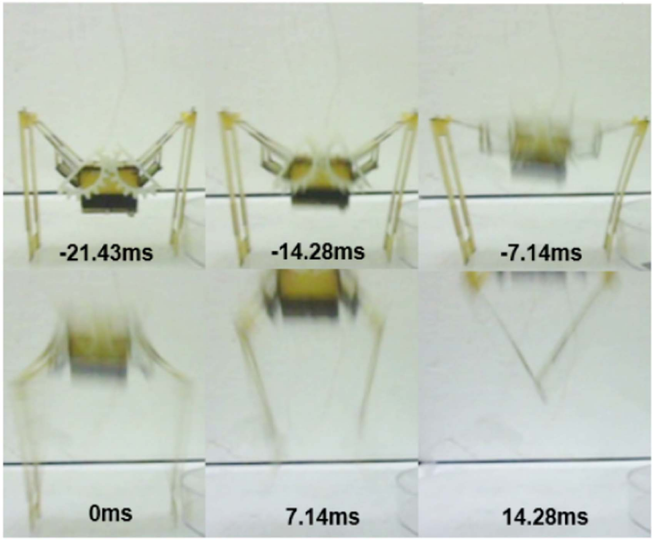

Figure 8. Close-up pictures of a synchronous upward jump. Zero ms is the moment of take-off. The angle between the tibia and the ground changes during the jumping process owing to the relatively long length of the femur.

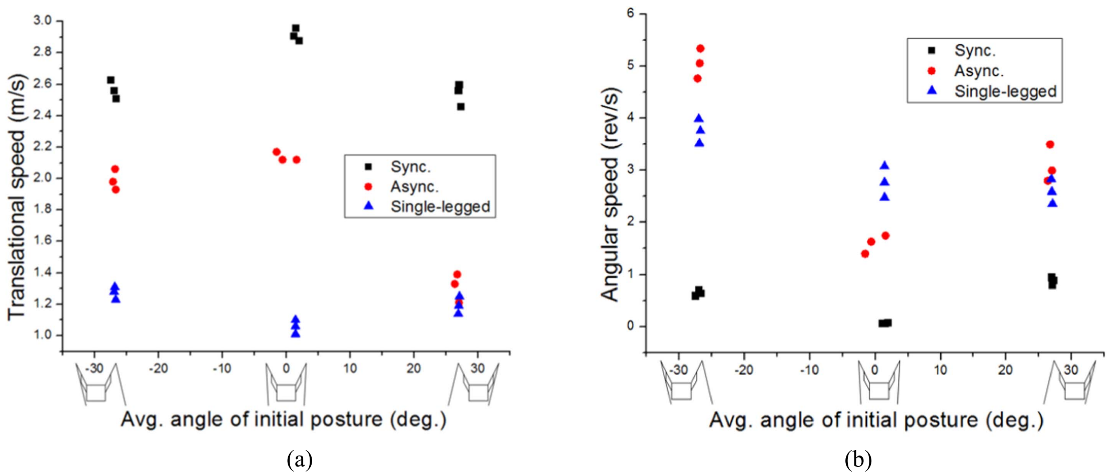

Figure 9. (a) Relation between take-off velocity and take-off average angle of initial posture. (a) Angular velocity versus average angle of initial posture.

jumps leftward, as shown in figure 7(b). Also, the maximum angle difference is about 9° in the asynchronous jump when the mechanism jumps rightward. In other directions, however, the jump direction does not change much. When the mechanism jumps upward, the jump directions of the three cases are not that different, although they all have a different rotating posture.

5.3. Jumping performance

As previously said, the type of jump (synchronous, asynchronous, or single-legged) does not really affect the jump direction. It does, however, influence jumping performance. Figures 10–12 show high-speed images of synchronous, asynchronous, and single-legged jumps, respectively. Overall, jumping direction corresponds to the average angle of the jumping legs, but there is a huge difference in translational and angular speed between the types of jump.

Figure 9 shows the take-off speed and the take-off angular speed for all three types of jump. The synchronous jumps show the highest take-off speed in all jumping directions. For example, when the mechanism jumps leftward, the synchronous jump has a speed of 2.57 m s^{-1} whereas the asynchronous jump has a speed of only 1.99 m s^{-1} and the single-legged jump has an even lower speed of 1.27 m s^{-1}. When the mechanism jumps rightward, similar differences are observed in general, but the asynchronous jump has a much decreased speed of 1.31 m s^{-1}, as shown in figure 9(a).

The speed reduction in the asynchronous jump and the single-legged jump occurs for the following two reasons. First, asynchronous and single-legged

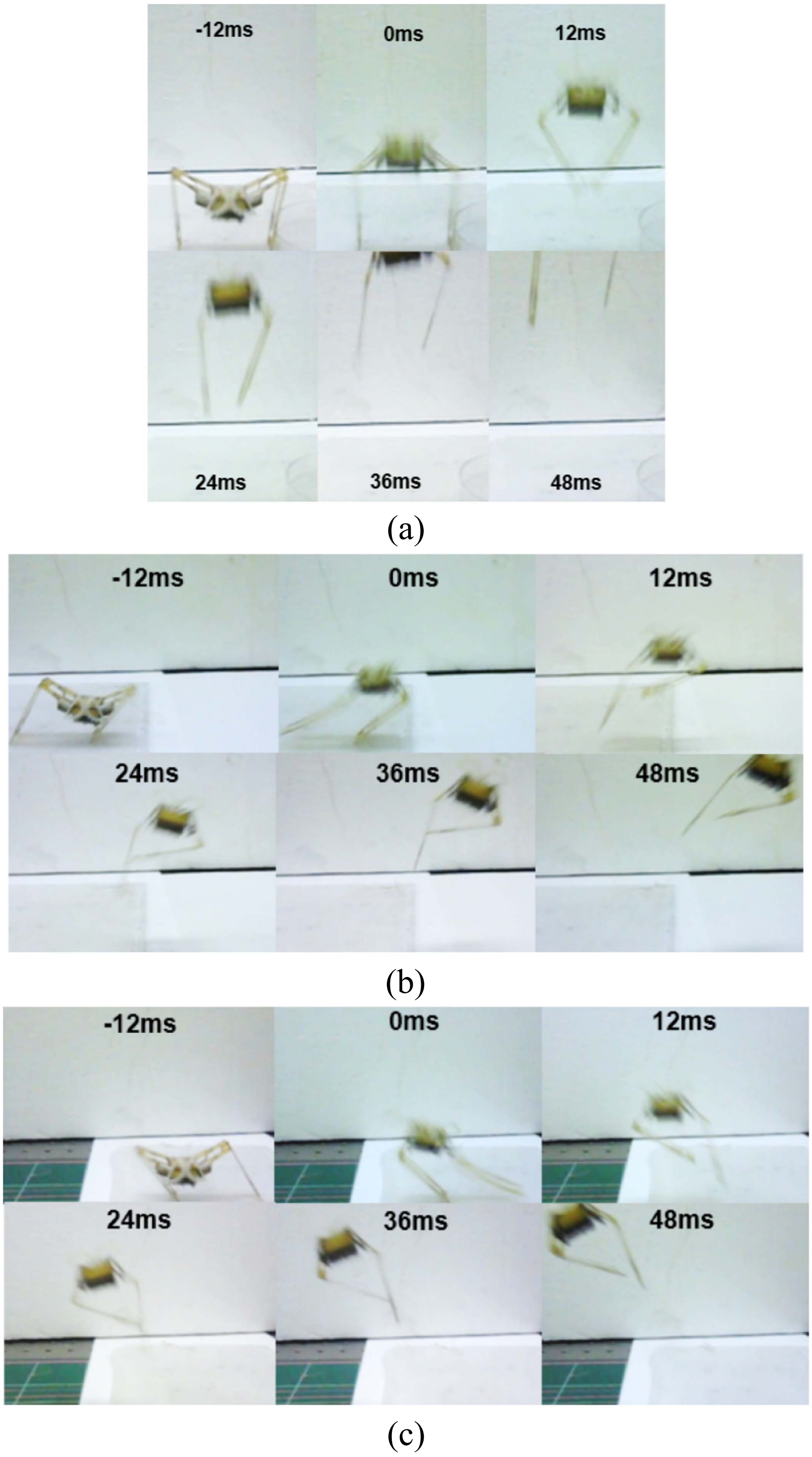

Figure 10. Synchronous jumping (a) upward, (b) rightward, and (c) leftward. Zero ms indicates the moment of take-off. The synchronous cases take off with reduced body rotation for various jumping directions.

jumps cannot fully use the initially stored energy. The single-legged jump basically utilizes half of the initially stored energy since it uses only one leg. In some asynchronous jumps, the delayed leg operates in the air since the first activated leg as already launched the mechanism. Therefore, the amount of transferred energy falls sharply, which causes speed to drop. Figure 11(b) corresponds to this case: the right leg operates first and propels the mechanism into the air, then the left leg operates.

The second reason concerns the increase in take-off angular speed, as shown in figure 9(b). Single-legged jumping has a take-off angular speed of 3.76 rev s^{-1} in the leftward direction, 2.78 rev s^{-1} in the upward direction, and 2.36 rev s^{-1} in the rightward direction. The asynchronous jump shows an angular speed of 5.05 rev s^{-1}, 1.59 rev s^{-1}, and

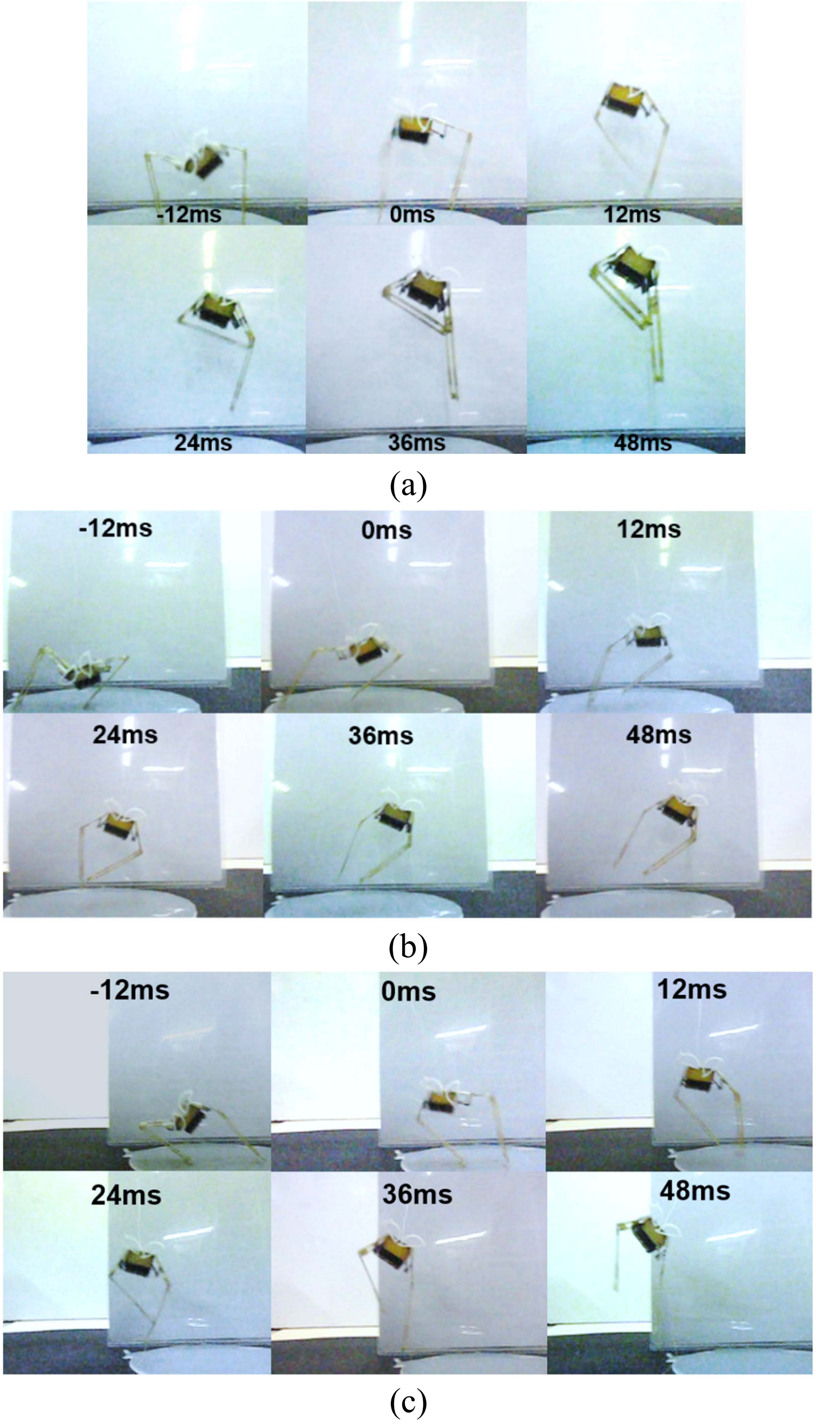

Figure 11. Asynchronous jumping (a) upward, (b) rightward, and (c) leftward. Zero ms indicates the moment of take-off. The activation timing difference of 14.2 ms always occurs owing to the specially designed gears. The left leg operates later, which causes the clockwise body spin.

3.11 rev s^{-1} in each direction. These values are much higher than those of the synchronous jumps, which tells us that some amount of energy is being transferred to body rotation, and that this phenomenon worsens as the mechanism changes jump direction. The synchronous jump, however, maintains low angular velocity even though the jump direction changes, and it shows high translational take-off velocity.

6. Discussion

Living things in nature are often sources of ideas for mechanical engineers who are seeking to design robots that can operate in unstructured environments. Just mimicking or copying biological mechanisms, however, is not important and is in fact almost impossible since they are way too complex for that. Instead, engineers need to consider living things as sources of

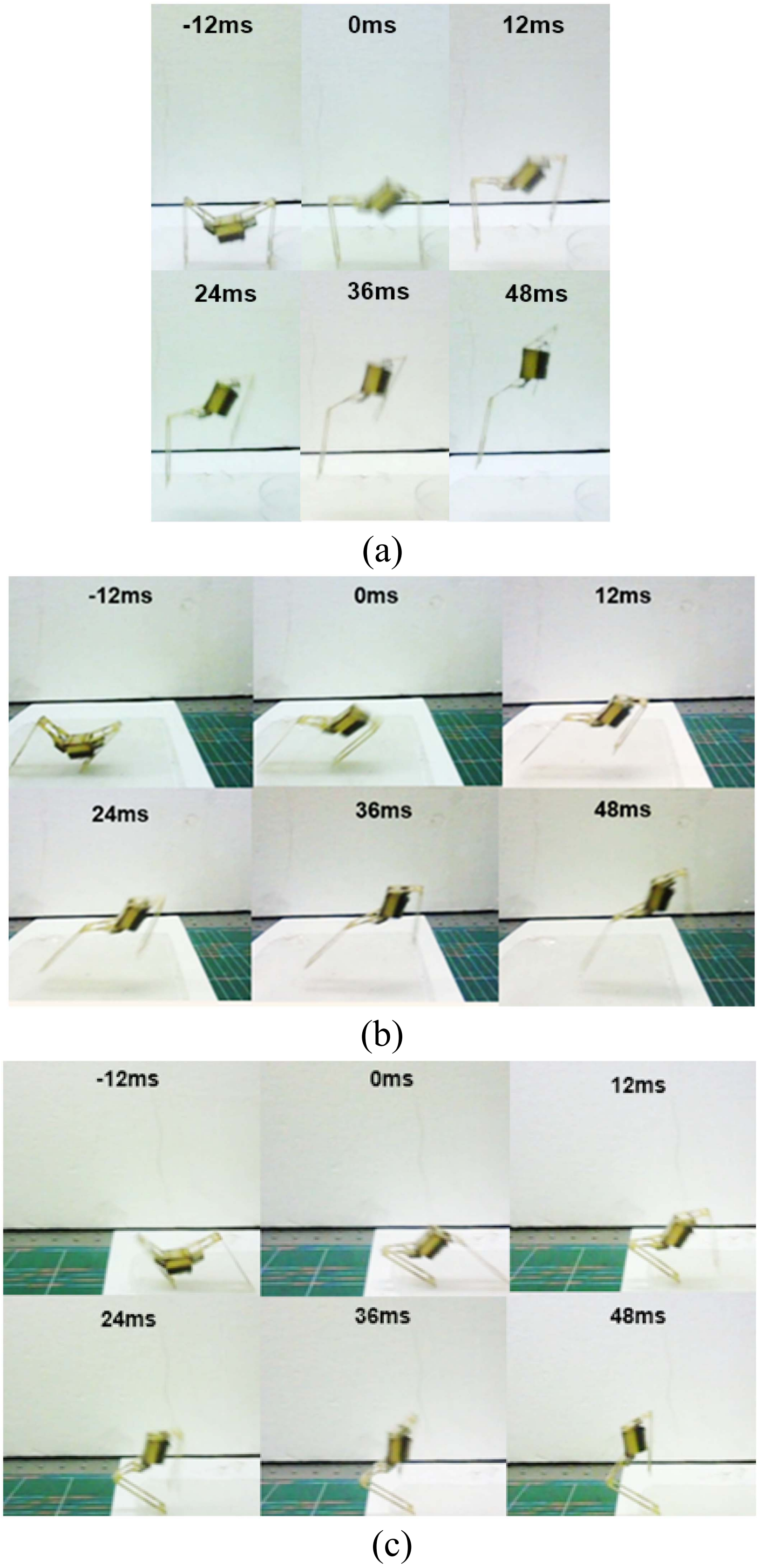

Figure 12. Single-legged jumping (a) upward, (b) rightward, and (c) leftward. Zero ms indicates the moment of take-off. The left leg is fixed so that it does not affect the right leg's jumping.

inspiration from which they can abstract novel principles. However, not all the principles involved in a particular biological mechanism need to be implemented since they may not all be helpful to the proposed concept. Only advantageous principles should be implemented to attain the best engineering solutions (Full 2005). That is how the authors approached this study—novel principles of steerable jumping were abstracted from the froghopper, and their essentials were investigated and translated into a mechanical engineering application

Most current jumping robots use independent structures to change jumping directions, and these tend to reduce jumping performance owing to the weight that they add. In contrast, the proposed concept does not incur a performance penalty because it is based on three principles derived from the way froghoppers are able to change their jumping direction without reduced jumping performance.

First, froghoppers use a pair of thrusting legs. It might seem trivial, but using two thrusters is the most important enabling technology for the froghopper. This idea inspired us to add not an additional direction-changing structure but one more thrusting leg. Two thrusting legs naturally boost the robot's jumping performance.

Second, froghoppers couple and synchronize their legs to reduce unnecessary body spin (Burrows and Sutton 2013). Froghoppers' thrusting legs are synchronized within 32 μs by means of gear-like structures on their trochanters. Similarly, gears are installed on both femurs of the proposed mechanism so that the robot's legs can operate simultaneously. In the experiments, this gearing method reduced unwanted body spin.

Third, froghoppers use a passive triggering method (Burrows 2006). Froghoppers engage the femur with a protrusion from the coxa in the fully levated position. When the force applied by the trochanteral depressor muscle is sufficient to overcome the resistance of the engagement, the hind legs suddenly and rapidly extend. This simple and effective method obviates the need for additional actuators. However, it is difficult to control the timing of this passive triggering method. The proposed concept uses a torque reversal mechanism to accomplish active triggering (Noh *et al* 2012). The torque reversal mechanism uses a separate SMA coil spring actuator for triggering. By activating the actuator, the mechanism can jump with the correct timing.

7. Conclusion

In this paper, we proposed a novel direction-changing concept and showed its potential use in miniature jumping robots. The proposed concept enables a robot to change jump direction with a minimal drop in jumping performance. The key design principles were inspired by the way froghoppers jump and consist of a pair of power-producing legs and moment cancellation via synchronized operation. To demonstrate the mechanism, several jumping tests were done by varying the initial posture, and the results show that the mechanism is able to change direction during synchronous jumping from $-40°$ to $40°$ with reduced body spin. Asynchronous and single-legged jumping were also tested to investigate how the lack of moment cancellation and synchronization affect jumping performance.

The proposed concept has only a limited range of changeable direction, but it still has the potential to improve the maneuverability and performance of miniature jumping robots. To apply this concept to a real jumping robot, future work should investigate using actuators to alter the initial posture and sensors to detect the posture of both tibiae since jumping direction is based on the average value of the posture of both tibiae.

Considering that the robot starts from layered manufacturing, low-profile actuators such as SMA actuators (Jung *et al* 2013, Koh *et al* 2014) or tendon-driven transmissions would suit the mechanism. One important constraint is that at the moment of take-off, the knee joints should freely rotate or have almost zero stiffness so that jumping direction may be precisely predicted based on the initial posture of the robot. If an SMA coil spring actuator is employed to meet this requirement, it needs to be designed so that a two-way shape memory effect is possible. After changing the initial angle by contracting the SMA coil spring, the SMA actuator needs to easily recover the relaxed state so as not to hinder operation of the knee joints during jumping. By antagonistically locating two SMA coil spring actuators with two-way shape memory effect, flexion and extension of the knee joint will be possible.

The other issue is how to measure the posture of both tibiae. Compass sensors could be appropriate for detecting the current posture of the tibiae because they can give information on the current azimuth of each tibia. In addition, off-the-shelf compass sensors are sub-milligram in weight and therefore would hardly affect the robot's mass. By using SMA coil spring actuators and compass sensors, the initial posture of the tibiae could be detected and the legs could be actuated to jump in the desired direction.

Acknowledgments

The authors thank Dr Gregory P Sutton for his permission to use figure 2 and Sun-Pill Jung for constructive discussions. This research was supported by a grant to the Bio-Mimetic Robot Research Center, funded by Defense Acquisition Program Administration under grant number UD130070ID.

References

Armour R, Paskins K, Bowyer A, Vincent J and Megill W 2007 Jumping robots: a biomimetic solution to locomotion across rough terrain *Bioinsp. Biomim.* **2** S65–82

Bartlett N W, Tolley M T, Overvelde J T, Weaver J C, Mosadegh B, Bertoldi K, Whitesides G M and Wood R J 2015 A 3D-printed, functionally graded soft robot powered by combustion *Science* **349** 161–5

Bennet-Clark H C 1975 The energetics of the jump of the locust Schistocerca gregaria *J. Exp. Biol.* **63** 53–83

Burdick J and Fiorini P 2003 Minimalist jumping robots for celestial exploration *Int. J. Robot. Res.* **22** 653–74

Burrows M 2003 Froghopper insects leap to new heights *Nature* **424** 509

Burrows M 2006 Morphology and action of the hind leg joints controlling jumping in froghopper insects *J. Exp. Biol.* **209** 4622–37

Burrows M and Sutton G 2013 Interacting gears synchronize propulsive leg movements in a jumping insect *Science* **341** 1254–6

Gerratt A P and Bergbreiter S 2013 Incorporating compliant elastomers for jumping locomotion in microrobots *Smart Mater. Struct.* **22** 014010

Jung G-P, Koh J-S and Cho K-J 2013 Underactuated adaptive gripper using flexural buckling *IEEE Trans. Robot.* **29** 1396–407

Koh J-S, Kim S-R and Cho K-J 2014 Self-folding origami using torsion shape memory alloy wire actuators *ASME 2014 Int. Design Engineering Technical Conf. and Computers and Information in Engineering Conf.*(American Society of Mechanical Engineers)

Koh J-S, Yang E, Jung G-P, Jung S-P, Son J H, Lee S-I, Jablonski P G, Wood R J, Kim H-Y and Cho K-J 2015 Jumping on water: surface tension—dominated jumping of water striders and robotic insects *Science* **349** 517–21

Kovac M, Fuchs M, Guignard A, Zufferey J-C and Floreano D 2008 A miniature 7 g jumping robot *IEEE Int. Conf. on Robotics and Automation (ICRA)* pp 373–8

Kovač M, Schlegel M, Zufferey J-C and Floreano D 2010 Steerable miniature jumping robot *Auton. Robots* **28** 295–306

Li F, Bonsignori G, Scarfogliero U, Chen D, Stefanini C, Liu W, Dario P and Fu X 2008 Jumping mini-robot with bioInspired legs *Proc. IEEE Int. Conf. on Robotics and Biomimetics* pp 933–8

Noh M, Kim S-W A S, Koh J-S and Cho K-J 2012 Flea-inspired catapult mechanism for miniature jumping robots *IEEE Trans. Robot.* **28** 1007–18

Stoeter S A, Rybski P E, Gini M and Papanikolopoulos N 2002 Autonomous stair-hopping with scout robots *IEEE/RSJ Int. Conf. on Intelligent Robots and Systems* (Piscataway, NJ: IEEE) pp 721–6

Sutton G P and Burrows M 2010 The mechanics of azimuth control in jumping by froghopper insects *J. Exp. Biol.* **213** 1406–16

Sutton G P and Burrows M 2011 Biomechanics of jumping in the flea *J. Exp. Biol.* **214** 836–47

Tolley M T, Shepherd R F, Karpelson M, Bartlett N W, Galloway K C, Wehner M, Nunes R, Whitesides G M and Wood R J 2014 An untethered jumping soft robot *2014 IEEE/RSJ Int. Conf. on Intelligent Robots and Systems (IROS 2014)* (Piscataway, NJ: IEEE) pp 561–6

Weiss P 2001 Hop… hop… hopbots!: designers of small, mobile robots take cues from grasshoppers and frogs *Sci. News* **159** 88–91

Wood R J, Avadhanula S, Sahai R, Steltz E and Fearing R S 2008 Microrobot design using fiber reinforced composites *J. Mech. Des.* **130** 052304

Woodward M A and Sitti M 2014 MultiMo-Bat: a biologically inspired integrated jumping-gliding robot *Int. J. Robot. Res.* **33** 1511–29

Zhao J, Yan W, Xi N, Mutka M W and Xiao L 2014 A miniature 25 grams running and jumping robot *ICRA*

Full R J 2005 The sticky wonder of Gecko feet *TED2005*